第 31 卷 第 2 期 无 机 材 料 学 报 Vol. 31 No. 2
2016 年 2 月 Journal of Inorganic Materials Feb., 2016

Article ID: 1000-324X(2016)02-0213-07 **DOI:** 10.15541/jim20150410

Investigation on Two Methods for Evaluating Mechanical Properties of Tube Materials

LIU Zhao[1], BAO Yi-Wang[1], WAN De-Tian[1], HU Chun-Lin[2], MA De-Long[1], TIAN Yuan[1]

(1. State Key Laboratory of Green Building Materials, China Building Materials Academy, Beijing 100024, China; 2. Department of Civil Engineering and Architecture, Wuhan University of Technology, Wuhan 430070, China)

Abstract: Elastic modulus and bending strength of tube materials were evaluated *via* compressing a split ring sample or a closed ring sample for different materials. Elastic modulus was estimated from the load-displacement relationship and sample dimensions in the range of elasticity, while bending strength was derived through the critical load at fracture. In this work, four tube materials were divided in two groups to research the applicable scopes of two methods. The results indicate that the split ring is suitable for materials with high brittleness and low limit strain, while the closed ring is available for low-stiffness materials. Comparison with the three-point bending data demonstrated the validity and convenience of two methods with the respective applicable range.

Key words: elastic modulus; bending strength; split ring; closed ring; tube materials

Tube materials have become one of anisotropic components that are commonly used[1-5] for both military fields (such as ejectors on the aircraft) and civil fields (such as water pipes underground or in the building). No matter where tube materials take service, their mechanical properties should be assessed primarily not only to ensure the safety during application but also to help predict their lifetime. Among these properties, elastic modulus and bending strength are two significant and acknowledged parameters for safe design and application of tube structures[6-8].

Over years, many methods have been proposed to evaluate elastic modulus and bending strength. The methods for evaluating elastic modulus can be generalized in two categories: static methods (bending method[9], tensile method[10] and indentation method[11]) and dynamic methods (impulse excited technique[12-13] and ultrasonic technique[14-15]). Meanwhile, three-point bending or four-point bending methods[9,16] are two most common approaches to estimate bending strength. However, most of these methods have the limitation of sample shape (rectangular beam) which are difficult and inconvenient for tube materials, especially for those with small or thin walls.

An efficient method has been proposed to solve the evaluating problems of brittle tube materials in our previous work, named the split ring method[17-18]. This method is quite appropriate to estimate brittle tube materials since an open ring sample possesses lower stiffness and greater deformation under a given load, compared with three-point bending samples. Experiments of ceramic and glass tube materials were performed and demonstrated the validity and reliability of the split ring method. Yet, for the tube materials with low stiffness, the results of this method would not be so accurate as those of high-stiffness samples because the required load was too small for common mechanical testing machine.

Regarding this limitation, the closed ring method was developed to evaluate the tube materials with low stiffness. Similar with the split ring method, elastic modulus could be obtained from the slope of load-displacement curve and sample dimensions. Bending strength would be calculated by critical load at fracture. In this paper, four common tube materials were considered and divided into two groups: high-stiffness group (alumina and quartz glass) and low-stiffness group (graphite and PMMA) to investigate the respective applicable scope. Additionally, the experiments of three-point bending method were performed to determine the reliability of both ring methods. Experimental results reveal two features: (i) For the split ring method, it is quite suitable to evaluate the brittle materials with high stiffness; (ii) For the closed ring method, it would be a significant supplement for the split ring

Received date: 2015-08-31; **Modified date:** 2015-09-25; **Published online:** 2015-11-20
Foundation item: National Natural Science Foundation of China (51172221, 51472227); Major Program of Scientific Instrument and Equipment Development of China (2011YQ140145); National High Technology Research and Development Program of China (863 Program, 2015AA034204)
Biography: LIU Zhao (1989–), male, candidate of Master degree. E-mail: liuzhao7945@163.com
Corresponding author: BAO Yi-Wang, professor. E-mail: ywbao@ctc.ac.cn

method, especially for materials with relatively high critical strain and low stiffness.

1 Basic principles

1.1 Split ring method

Based on Castigliano's second theorey, if the split ring is loaded within the range of elasticity (Fig. 1), elastic modulus can be calculated[17],

$$E=\frac{3\pi}{4000b}\frac{\Delta P}{\Delta\delta}\frac{\left(R+r\right)^3}{\left(R-r\right)^3} \tag{1}$$

Where E is the elastic modulus, GPa; ΔP is the load increment, N; $\Delta\delta$ is the displacement increment, mm; R is the outer radius, mm; r is the inner radius, mm; b is the width, mm.

If keep loading the split ring until fracture (starting from point A, the maximum tensile stress point on the whole split ring), the bending strength will be obtained[17],

$$\sigma=\frac{P_c}{bR\left(\ln(R/r)\dfrac{R+r}{R-r}-2\right)} \tag{2}$$

Where σ is the bending strength, MPa; P_c is the critical load, N.

1.2 Closed ring method

1.2.1 Elastic modulus

Figure 2 shows the schematic structure of the closed ring during loading. According to mechanics of materials[19], the bending moment M at any cross section of the closed ring can be expressed,

$$M=\frac{1}{2}P\left(R+r\right)\left(\frac{\sin\theta}{2}-\frac{1}{\pi}\right) \tag{3}$$

Where P is the applied load, θ is the angle between the cross section and the vertical line.

Order partial derivative of bending moment M with respect to load P,

$$\frac{\partial M}{\partial P}=\frac{1}{2}\left(R+r\right)\left(\frac{\sin\theta}{2}-\frac{1}{\pi}\right) \tag{4}$$

On the basis of the Castigliano's second theorem[20], if just consider half of the closed ring for the symmetry, that is $\theta\in[0,\pi]$, the vertical displacement within elasticity will be derived,

$$\Delta\delta'=\int\frac{M}{EI}\times\frac{\partial M}{\partial P}\mathrm{d}s=\frac{1}{8EI}\int_0^{\pi}P\left(R+r\right)^3\left(\frac{\sin\theta}{2}-\frac{1}{\pi}\right)^2 \mathrm{d}\theta=\frac{\left(\pi^2-8\right)\Delta P\left(R+r\right)^3}{64\pi EI} \tag{5}$$

Where I is inertia moment and $I=b\left(R-r\right)^3/12$ for the cross section of the closed ring.

Notably, the establishment of Eq. (5) is dependent on the case of the tube materials with thin wall, *viz*. the ratio of $R+r$ to $R-r$ should be above 10. The tube materials with thick wall are not studied and discussed in this work.

The total displacement of the closed ring $\Delta\delta$ will be twice of $\Delta\delta'$, that is $\Delta\delta=2\Delta\delta'$. Thus, if the unit of ΔP is N, the unit of E is GPa, the units of R, r and b are mm, elastic modulus E in Eq. (5) can be written in the following form,

$$E=\frac{3\left(\pi^2-8\right)}{8000\pi b}\times\frac{\Delta P}{\Delta\delta}\times\left(\frac{R+r}{R-r}\right)^3 \tag{6}$$

Where $\Delta P/\Delta\delta$ is the slope of load-displacement curve within elasticity, N/mm.

1.2.2 Bending strength

Based on mechanics of materials[19], the direct stress of pure bending for stress point at any cross section of the plane curved bar is

$$\sigma=\frac{My}{S\xi} \tag{7}$$

Where y is the distance from the stress point to the neutral axis; S is the static moment of the total cross section to the neutral axis; ξ is the distance between the stress point and the center of curvature.

When the closed ring is failure under a compressive load, the facture must be originated from point B and B' without any axial force or shearing force, both are the maximum tensile stress points on the whole ring (actually, facture at two points hardly occur simultaneously). Here, we take point B into account in Fig. 2.

As the longitudinal symmetry section of point B magnified in Fig. 3, M, y, S and ξ can be obtained from mechanics of materials as follows[19],

$$M=-\frac{1}{2\pi}P\left(R+r\right) \tag{8}$$

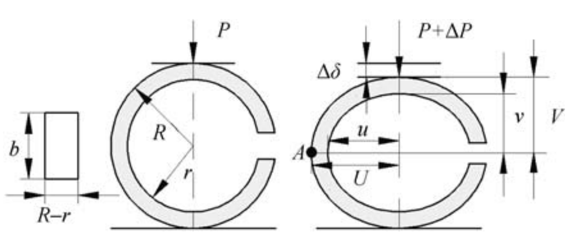

Fig. 1 Schematic of the split ring before and during loading

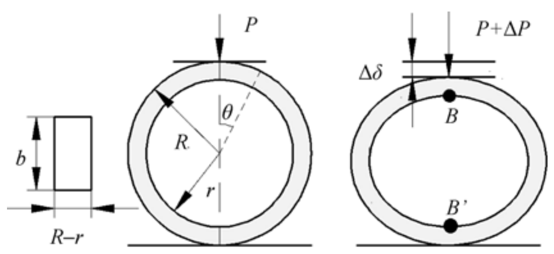

Fig. 2 Schematic of the closed ring before and during loading

$$y = r - \frac{R-r}{\ln(R/r)} \tag{9}$$

$$S = b(R-r)\left[\frac{R+r}{2} - \frac{R-r}{\ln(R/r)}\right] \tag{10}$$

$$\xi = r \tag{11}$$

Substitute Eq. (8)-(11) into Eq. (7) and change the form,

$$\sigma = \frac{P_c\left(1-\frac{\ln a}{a-1}\right)}{\pi br\left[\ln a - \frac{2(a-1)}{a+1}\right]} \tag{12}$$

Where a is the ratio of radius and $a = R/r$.

2 Material and experimental procedure

Four tube materials were selected in this test: alumina, quartz glass, graphite and polymethyl methacrylate (PMMA), with some basic information shown in Table 1. First, the ring samples would be cut from tube materials, with width of 8 mm. Next, all the samples should be ground on the surface and chamfered. Then, a split was spliced on the ring sample as shown in Fig. 4. The related dimensions were measured by a vernier caliper with the precision of 0.02 mm. In addition, a set of three-point bending samples (Fig. 4) were machined on the basis of ASTM C120/ C120M–12[21]. The dimension of the sample was 60 mm×10 mm×5 mm (length×width×thickness), with the support span of 50 mm. For the sake of brevity, the methods used in this work were renamed as “C” method, “O” method and “3” method in section 4.

All the loading experiments were carried out by the universal mechanical testing machine (MTS, CMT 5105, China). The crosshead speeds for modulus test and strength test were shown in Table 2. Particularly, the displacement of samples in the modulus test was measured by the accurate inductance measuring instrument (MT 220, China) with the precision of 1 μm. At least five samples should be tested by each method to obtain an average modulus or strength value.

3 Results and discussion

3.1 Elastic modulus

3.1.1 High-stiffness group

Figure 5 shows elastic modulus of alumina and quartz glass measured by “C” method, “O” method and “3” method. The values of E_c/E_3 and E_o/E_3 were used to assess the accuracy of both “C” method and “O” method, where E_c, E_o and E_3 represented the elastic modulus

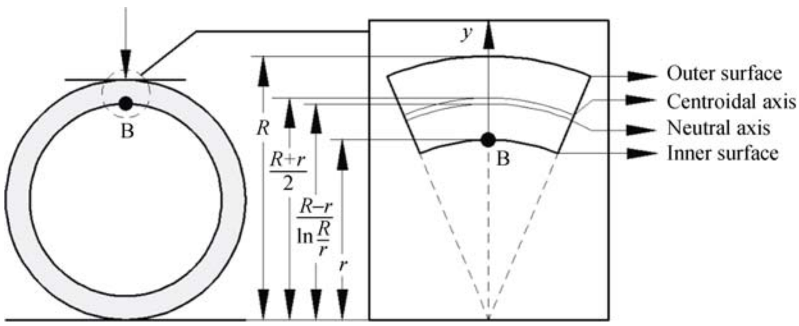

Fig. 3 Schematic of the longitudinal symmetry section at stress point B

Table 1 Components, physical properties and dimensions of four testing tube materials

Sample	Gradients & Contents /%	Density /(g·cm^{-3})	Thermal expansion coefficient /(×10^{-6}, K^{-1})	Thermal conductivity /(W·m^{-1}·K^{-1})	Size/mm	
					R	r
Alumina	Al_2O_3: 99.70	3.67	8.60	25.00	15	12
Quartz glass	SiO_2: 99.95	2.26	0.55	41.00	24	21
Graphite	C: 99.92	1.83	4.30	106.00	15	12
PMMA	PMMA: 100.00	1.18	85.00	0.19	18	15

Table 2 Loading speeds for modulus test and strength test

Loading speed /(mm·min^{-1})	Alumina		Quartz glass		Graphite		PMMA	
	E	σ	E	σ	E	σ	E	σ
Split ring test (C)	0.10	0.5	0.10	0.5	0.2	1.0	0.5	2.5
Closed ring test (O)	0.02	0.1	0.04	0.2	0.1	0.5	0.4	2.0
Three-point bending test (3)	0.02	0.1	0.04	0.2	0.1	0.5	0.4	2.0

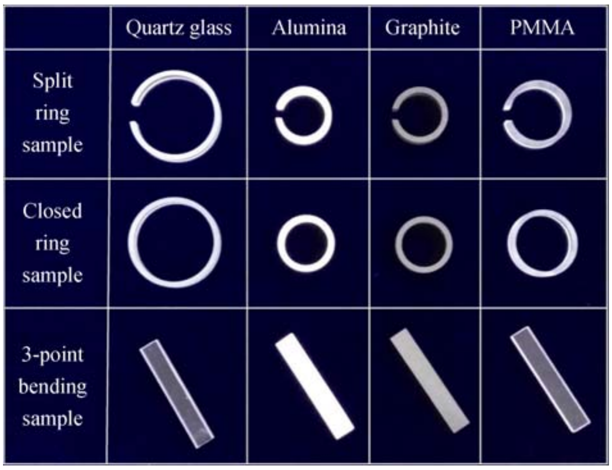

Fig. 4 Photograph of testing samples used in this work

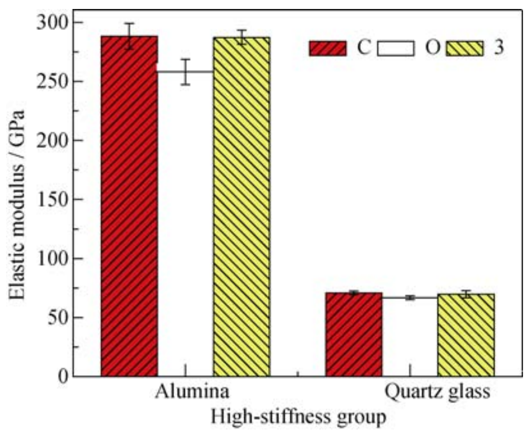

Fig. 5 Elastic modulus of high-stiffness group measured by three methods

Table 3 The ratio of modulus for four tube materials

Sample	Alumina	Quartz glass	Graphite	PMMA
E_c/E_3	1.003	1.007	1.024	1.095
E_o/E_3	0.898	0.956	1.014	1.007

measured by "C" method, "O" method and "3" method, respectively. It was apparent that E_c/E_3 and E_o/E_3 were within the reasonable range (1 ± 5%) except the value of 0.898 (Table 3). This partial small modulus obtained from "O" method was due to the displacement measurement, which excessed the precision range of inductance measuring instrument that even the deviation of 1 μm would make a big effect on the calculated result. Even so, it didn't mean that "O" method was invalid to evaluate elastic modulus like alumina, but not so accurate as "C" method. When the stiffness decreased to the level of quartz glass, the data of "C" method and "O" method were basically close to the values measured by "3" method.

3.1.2 Low-stiffness group

Similar with high-stiffness group, there was also a little deviated value among the results of low-stiffness group (Fig. 6), the modulus of PMMA estimated by "C" method. It resulted from the accuracy of load measurement. The displacement of a split ring sample like PMMA would be quite large so that the load increment ΔP had to be adjusted to a minor value that would excess the accuracy of loading system. Obviously, compared with the results of high-stiffness group, both "C" method and "O" method would be suitable to evaluate elastic modulus of tube materials regardless of high stiffness or not, as long as the measurements of load and displacement were accurate enough.

3.2 Bending Strength

3.2.1 High-stiffness group

Based on the Weibull statistical theory[22-23], "3" method is suitable and satisfactory to compare and analyze the strength evaluated by "C" method and "O" method for two reasons. First, the failures of three types of samples are belonged to bending fracture and occur at the point of the maximum tensile stress, with the similar effective Weibull volumes for all these methods. That means there should be not much difference among the strength values tested by three methods. Second, "3" method possesses the relatively wide range for strength measurement due to its convenience in sample preparation. Thus, "3" method is selected to test and verify "C" method and "O" method and provide their applicable ranges for reference.

Furthermore, it is worth noting the basic two premises for the strength calculation in this work: (i) the samples should be brittle failure without any yield stage (such as the four samples selected in this test); (ii) the maximum compressive displacement would not be too large that the original dimensions were not suitable at fracture. The second premise was the primary factor for these two methods to be applied or not. Therefore, the ultimate strain ε_b has been introduced to take the deformation into account, which equals to the ratio of bending strength and elastic modulus,

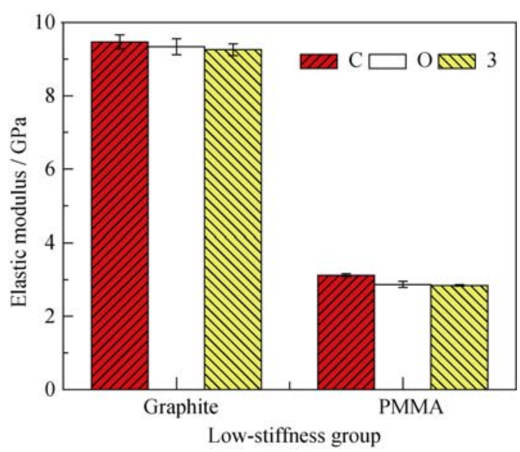

Fig. 6 Elastic modulus of low-stiffness group measured by three methods

$$\varepsilon_b = \frac{\sigma}{E} \quad (13)$$

The elastic modulus to calculate ε_b would use the results of "3" method uniformly for all the samples ($\varepsilon_{bi} = \sigma_i / E_3$, i=c, o, 3). For the high-stiffness group (Table 4), the values of $\varepsilon_{bc}/\varepsilon_{b3}$ and $\varepsilon_{bo}/\varepsilon_{b3}$ were within the acceptable error range (1±5%). That meant both methods were excellent choices to evaluate bending strength of the tube materials such as alumina and quartz glass (Fig. 7). It was inferred that whether "C" method or "O" method could be valid was based on the value of ε_b.

3.2.2 Low-stiffness group

Figure 8 displays bending strength of graphite and PMMA measured by three methods. It could be seen that "C" method was not applicable due to the huge displacement at fracture (the split ring sample of PMMA even didn't fracture until the split closed). To confirm the applicable ranges of strength evaluation for both "C" method and "O" method, the relationship between ε_{b3} and $\varepsilon_b/\varepsilon_{b3}$ was plotted in Fig. 9. If the maximum acceptable error range was set as ± 5%, the available values of ε_{b3} should not excess 3.81×10^{-3} for "C" method and 14.66×10^{-3} for "O" method, respectively. Thus, before evaluating bending strength, the approximate value of ε_b should be realized first to decide which method would be available.

Obviously as it is, if ε_b excessed the upper limit value as mentioned above, such large deformation would make the calculated strength value deviated. Here, an approximate value of bending strength would be proposed through taking the split ring sample of graphite as an example. The shape of sample was transformed into an ellipse at fracture, of which semi-axes were shown in Fig. 1

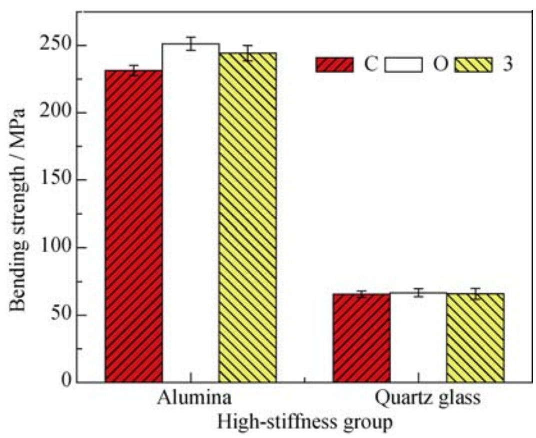

Fig. 7　Bending strength of high-stiffness group measured by three methods

Table 4　The ratio of the ultimate strain for four tube materials

Sample	Alumina	Quartz glass	Graphite	PMMA
$\varepsilon_{bc}/\varepsilon_{b3}$	0.955	0.996	0.910	–
$\varepsilon_{bo}/\varepsilon_{b3}$	1.027	1.012	0.992	0.843

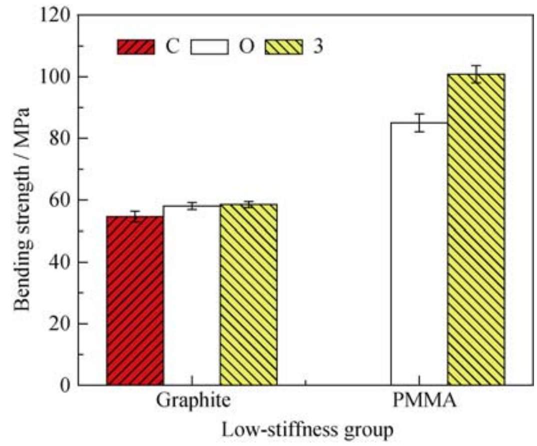

Fig. 8　Bending strength of low-stiffness group measured by three methods

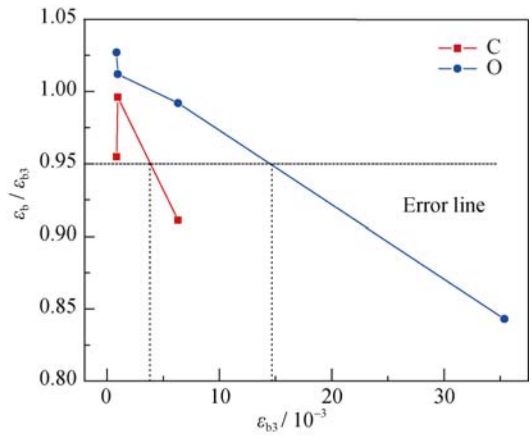

Fig. 9　The relationship between ε_{b3} and $\varepsilon_b/\varepsilon_{b3}$ for both methods

(here P=0, P+ΔP=P_c and $\Delta\delta = \delta_c$). Particularly, two hypotheses were helpful to solve this problem easily: (i) the thickness of the sample ($R - r$) was constant until fracture; (ii) the circumference of ellipse sample was also constant, equal to the original circle. Thus, the values of major semi-axis and minor semi-axis could be obtained,

$$V = R - \delta_c \quad (14)$$

$$U = \frac{\pi(R - V)}{2} + V \quad (15)$$

$$u = U - (R - r) \quad (16)$$

Where δ_c is the maximum compressive displacement, mm; V is the minor semi-axis of outer ellipse, mm; U is the major semi-axis of outer ellipse, mm; u is the major semi-axis of inner ellipse, mm.

U and u would be substitute into Eq. (2) to replace R and r, respectively. For the split ring sample of graphite, P_c was 52.23 N and δ_c was 2.56 mm. Based on Eq. (14)- (16) and Eq. (12), the modified strength value was 58.81 MPa, which was nearly access to the results measured by "3" method (58.51 MPa). The closed ring sample of PMMA could be calibrated in the same way. However, the accurate analysis formula for large deformation would introduce the geometric non-linearity, which might be discussed in the future work.

4 Conclusions

Elastic modulus and bending strength of tube materials have been solved by using the split ring method and the closed ring method, through deriving the slope of load-displacement curve and the critical load at fracture. The experimental results with four kinds of tube materials demonstrated the excellent accuracy and reliability compared with three-point bending method. Main conclusions from this work are drawn as below:

1) It is proposed that elastic modulus of the tube materials with high stiffness should be evaluated by the split ring, while the closed ring is suitable to estimate the tube materials with low stiffness.

2) For bending strength, the ultimate strain ε_b is rather important and useful to distinguish the applicable ranges for both ring methods. In terms of machining difficulty, the split ring method is suggested to estimate brittle materials while the closed ring method is suitable for quasi-brittle materials.

3) Above all, the closed ring method is a significant complementary approach for the split ring method, with more easily prepared samples. Based on these two methods, it is inferred that the mechanical behaviors of tube materials under some special conditions may be evaluated in the subsequent work, such as extreme environments or coatings on tube materials.

References:

[1] JAHANBAKHSH A, HAGHGOU H R, ALIZADEH S. Experimental analysis of a heat pipe operated solar collector using water–ethanol solution as the working fluid. *Sol. Energy*, 2015, **118:** 267–275.

[2] NAOUM-SAWAYA J, GHADDAR B, ARANDIA E, *et al.* Simulation-optimization approaches for water pump scheduling and pipe replacement problems. *Eur. J. Oper. Res.*, 2015, **246(1):** 293–306.

[3] RYSSEL S T, ARVIN E, LÜTZHØFT H H, *et al*. Degradation of specific aromatic compounds migrating from PEX pipes into drinking water. *Water Res.*, 2015, **81:** 269–278.

[4] YU W B, LIU W B, LAI Y M, *et al*. Nonlinear analysis of coupled temperature-seepage problem of warm oil pipe in permafrost regions of Northeast China. *Appl. Therm. Eng.*, 2014, **70(1):** 988–995.

[5] RIAÑO A B, RODRIGUEZ I H, BANNWART A C, *et al*. Film thickness measurement in oil–water pipe flow using image processing technique. *Exp. Therm. Fluid Sci.*, 2015, **68:** 330–338.

[6] YOSHIMURA H N, GONZAGA C C, CESAR P F, *et al*. Relationship between elastic and mechanical properties of dental ceramics and their index of brittleness. *Ceram. Int.*, 2012, **38(6):** 4715–4722.

[7] ZHOU J Q, LI Y L, ZHU R T, *et al*. The grain size and porosity dependent elastic moduli and yield strength of nanocrystalline ceramics. *Mater. Sci. Eng. A*, 2007, **445:** 717–724.

[8] FAN X, CASE E D, REN F, *et al*. Part II: Fracture strength and elastic modulus as a function of porosity for hydroxyapatite and other brittle materials. *J. Mech. Behav. Biomed. Mater.*, 2012, **8:** 99–110.

[9] MUJIKA F. On the difference between flexural moduli obtained by three-point and four-point bending tests. *Polym. Test.*, 2006, **25:** 214–220.

[10] NEUMAN E W, HILMAS G E, FAHRENHOLTZ W G. Mechanical behavior of zirconium diboride–silicon carbide ceramics at elevated temperature in air. *J. Eur. Ceram. Soc.*, 2013, **33(15):** 2889–2899.

[11] SÁNCHEZ-GONZÁLEZ E, MIRANDA P, MEI LÉNDEZ-MARTÍNEZ J J, *et al*. Temperature dependence of mechanical properties of alumina up to the onset of creep. *J. Eur. Ceram. Soc.*, 2007, **27(11):** 3345–3349.

[12] SIBIL A, ERAUW J P, CAMBIER F, *et al*. Study of damage of high zirconia fused-cast refractories by measurement of Young's modulus. *Mater. Sci. Eng. A*, 2009, **521:** 221–223.

[13] WOLFENDEN A, KURY P B, PETROVIC J J. Measurement of dynamic Young's modulus for molybdenum disilicide/pentatitanium trisilicide. *J. Mater. Eng. Perform.*, 1996, **5(2):** 232–234.

[14] LUZ A P, HUGER M, PANDOLFELLI V C. Hot elastic modulus of Al_2O_3–SiC–SiO_2–C castables. *Ceram. Int.*, 2011, **37(7):** 2335–2345.

[15] CHI Y S, SHEN J Y, CHEN X X, *et al*. Elastic moduli of MgO-Al_2O_3-SiO_2-TiO_2-Y_2O_3 glass. *J. Inorg. Mater.*, 2002, **17(3):** 475–479.

[16] BENSALAH W, FEKI M, DE-PETRIS WERY M, *et al*. Optimization of the 3-Point bending failure of anodized aluminum formed in tartaric/sulphuric acid using doehlert design. *J. Mater. Eng. Perform.*, 2015, **24(2):** 737–747.

[17] Test Method for Determining Elastic Modulus and Bending Strength of Ceramic Tube and Rings, Fine Ceramics (Advanced Ceramics, Advanced Technological Ceramics). ISO 18558, 2015.

[18] LIU Z, BAO Y W, WEI C G, *et al*. Evaluation of elastic modulus of quartz glass tube at high temperature by modified split ring method. *J. Inorg. Mater.*, 2015, **30(8):** 838–842.

[19] BEER F, JOHNSTON R. Mechanics of Materials, sixth edition. America: McGraw-Hill, 2012.

[20] MIRANDA P, PAJARES A, GUIBERTEAU F, *et al*. Role of flaw statistics in contact fracture of brittle coatings. *Acta Mater.*, 2001, **49(18):** 3719–3726.

[21] Standard Test Methods of Flexure Testing of Slate (Breaking Load, Modulus of Rupture, Modulus of Elasticity), C120/C120M – 12, ASTM, West Conshohocken, PA, USA, 2012.

[22] QUINN G D. Weibull effective volumes and surfaces for cylindrical rods loaded in flexure. *J. Am. Ceram. Soc.*, 2003, **86(3):** 475–479.

[23] BAO Y W, ZHOU Y C, ZHANG H B. Investigation on reliability of nanolayer-grained Ti_3SiC_2 *via* Weibull statistics. *J. Mater. Sci.*, 2007, **42(12):** 4470–4475.

两种方法评价管材力学性能的研究

刘 钊[1], 包亦望[1], 万德田[1], 胡春林[2], 马德隆[1], 田 远[1]

(1. 中国建筑材料科学研究总院 绿色建材国家重点实验室, 北京 100024; 2. 武汉理工大学 土木工程与建筑学院, 武汉 430070)

摘 要: 通过挤压一个缺口环或闭口环样品来评价不同管材的弹性模量和弯曲强度。在弹性范围内, 弹性模量可由载荷—位移关系和样品尺寸获到; 而弯曲强度则由断裂临界载荷决定。在本研究中, 四种管材被分为两组来研究这两种方法的适用范围。结果表明: 缺口环适合评价刚度较大、极限应变较小的材料, 而闭口环则更倾向于评价低刚度的材料。此外, 三点弯曲的数据也验证了这两种方法的有效性、便捷性及其各自的适用范围。

关 键 词: 弹性模量; 弯曲强度; 缺口环; 闭口环; 管材

中图分类号: TQ174 **文献标识码:** A